# REPORT DOCUMENTATION PAGE

Form Approved
OMB No. 0704-0188



| 1. AGENCY USE ONLY (Leave blank) | 2. REPORT DATE | 3. REPORT TYPE AND DATES COVERED |
|---|---|---|
| | | FINAL TECHNICAL REPORT-15 Jun 92-14 Dec |

4. TITLE AND SUBTITLE
Millimeter-Wave Network Analysis and Spectrosocpy

5. FUNDING NUMBERS
61103D
3484/S3

6. AUTHOR(S)
Professor Mark Rodwell

7. PERFORMING ORGANIZATION NAME(S) AND ADDRESS(ES)
Department of Electrical and Computer Engineering
University of California
Santa Barbara, CA 93106

8. PERFORMING ORGANIZATION REPORT NUMBER
AFOSR-TR-
96-0042

9. SPONSORING/MONITORING AGENCY NAME(S) AND ADDRESS(ES)
AFOSR/NE
110 Duncan Avenue Suite B115
Bolling AFB DC 20332-0001

10. SPONSORING/MONITORING AGENCY REPORT NUMBER
F49620-92-J-0365

11. SUPPLEMENTARY NOTES

12a. DISTRIBUTION/AVAILABILITY STATEMENT
APPROVED FOR PUBLIC RELEASE: DISTRIBUTION UNLIMITED

12b. DISTRIBUTION CODE

## Abstract

In the program "Millimeter-Wave Network Analysis and Spectroscopy with Solid-State Devices", AFOSR/AASERT grant #F49620-92-J-~~0469~~ 0365 (associated with the AFOSR parent grant #F49620-92-J-0469) the following devices have been developed and experimental results obtained:

- Shock-wave nonlinear-transmission-line (NLTL) pulse generators and NLTL-gated sampling circuits have been built with 0.48 ps risetimes and 725 GHz bandwidths.

- Development of 500-100 GHz Schottky-collector Heterojunction Bipolar Transistors were pursued, including device design, mask layout, and two generations of devices fabricated. At the time of the contract end, devices with 120 GHz bandwidths were obtained.

- Active probes (using NLTL technologies) have been constructed for on-wafer mm-wave network analysis, and measurements demonstrated over a 10-200 GHz bandwidth. The system was then demonstrated with extensive measurements of advanced high-speed ICs.

14. PAGES

16. PRICE CODE

| 17. SECURITY CLASSIFICATION OF REPORT | 18. SECURITY CLASSIFICATION OF THIS PAGE | 19. SECURITY CLASSIFICATION OF ABSTRACT | 20. LIMITATION OF ABSTRACT |
|---|---|---|---|
| UNCLASSIFIED | UNCLASSIFIED | UNCLASSIFIED | |

# FINAL TECHNICAL REPORT

## 15 June 1992 - 14 December 1995

## F49620-92-J-0365

# Millimeter-Wave Network Analysis and Spectroscopy

Professor Mark Rodwell
Department of Electrical and Computer Engineering
University of California
Santa Barbara, CA 93106

**Abstract**

In the program "Millimeter-Wave Network Analysis and Spectroscopy with Solid-State Devices", AFOSR/AASERT grant #F49620-92-J-~~0469~~ 0365 (associated with the AFOSR parent grant #F49620-92-J-0469) the following devices have been developed and experimental results obtained:

- Shock-wave nonlinear-transmission-line (NLTL) pulse generators and NLTL-gated sampling circuits have been built with 0.48 ps risetimes and 725 GHz bandwidths.

- Development of 500-100 GHz Schottky-collector Heterojunction Bipolar Transistors were pursued, including device design, mask layout, and two generations of devices fabricated. At the time of the contract end, devices with 120 GHz bandwidths were obtained.

- Active probes (using NLTL technologies) have been constructed for on-wafer mm-wave network analysis, and measurements demonstrated over a 10-200 GHz bandwidth. The system was then demonstrated with extensive measurements of advanced high-speed ICs.

## TABLE OF CONTENTS


| Item | Page |
|---|---|
| Research Accomplishments | 3 |
| 0.48 ps (725 GHz) pulse generators and sampling circuits | 3 |
| Schottky-collector Bipolar Transistors | 7 |
| Technical Description | 7 |
| Progress during the reported contract period | 10 |
| Active Probes for on-wafer electrical measurements to 200 GHz | 17 |
| List of Personnel and Degrees | 23 |
| Consulting and Advisory Functions | 23 |
| Inventions and Patent Disclosures | 23 |
| List of Written Publications in Technical Journals | 23 |
| Papers Presented at Conferences | 24 |

## Research Accomplishments

0.48 ps (725 GHz) pulse generators and sampling circuits

A primary goal of the program was extension of NLTL pulse generator and sampling circuit bandwidths. At the time of program initiation, NLTLs and their related sampling circuits had 1.3 ps transition times, corresponding to 275 GHz bandwidths. At the time of the last program report, at 9/20/93, we had extended NLTL and sampling circuit bandwidths to 515 GHz and obtained 0.68 ps deconvolved transients from NLTLs. During the period covered in the present report, after extensive efforts, NLTL pulse risetimes were reduced to 0.48 ps and NLTL-gated sampling circuits increased to DC-725 GHz bandwidths.

Work pursued in order to obtain the 725 GHz / 0.48 ps result is described below. At the bandwidths involved, the circuit dimensions and device spacings approach the dimensions of the devices themselves. The metal lines interconnecting the devices no longer behave as ideal transmission lines and have substantial parasitics. On the earlier 515 GHz NLTLs, layout capacitance was severe, decreasing the compression of the high-frequency portions of the device by almost 30%. To compensate for the reduced compression per unit length, the NLTL length had to be increased, which increased the NLTL's attenuation, further impairing performance.

To reduce layout parasitics, the NLTLs transverse dimensions must small compared to a wavelength of the highest Fourier component of the signal. Signal line conductors on the 0.68 ps NLTLs were only 5 μm wide over a 1 mm distance; this resulted in very high skin loss. The signal deviation near the NLTL output was thus reduced, and did not encompass the range between zero and -2 Volts where the diode capacitance varies most strongly. This reduced the NLTL's dynamic compression, increasing the falltime of the generated shock wavefronts. Given high attenuation, large input drive must be used, and the diodes must have high breakdown voltages and hence low cutoff frequencies.

Bandwidth of the 515 GHz / 0.68 ps NLTL was limited primarily by transmission-line parasitics and attenuation. In order to extend the NLTL bandwidth, the 725 GHz / 0.48 ps NLTLs developed in the present contract period used elevated coplanar waveguide. Elevated coplanar waveguide is a transmission line in which the metal signal conductor is raised 2 μm above the semiconductor substrate. Fabrication processes for elevated CPW are an extension of air-bridge fabrication processes. Air-dielectric transmission lines were used to a limited extent by the Stanford group at the input sections of their NLTLs; it is however near the NLTL output, with its small diode spacings, very high skin-effect losses, and high Bragg frequencies where the air-bridge-lines have the most significant impact.

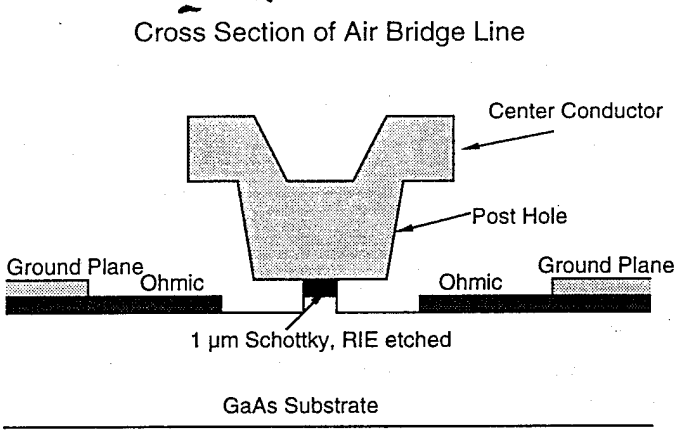


Figure 1: Cross-section of the elevated coplanar waveguide NLTL .

The air-bridge-line is a coplanar waveguide (CPW) transmission line with the signal conductor raised above the semiconductor (dielectric) surface. Because the field is primarily in air rather than the GaAs substrate, the line's effective dielectric constant is reduced from 7 to 1.1. The electrical velocity is increased, permitting higher Bragg frequencies, and wider conductors can be used, reducing skin loss.

| Design Parameter | 515 GHz design (last report) | 725 GHz design (this report) |
|---|---|---|
| Line Loss | 8 dB | 3.8 dB |
| Diode Doping | $10^{17}$ | several designs |
| Loss Compensation | Gradient Biasing | Impedance Tapering |
| Expected Edge Speed (SPICE) | 0.60 ps | 0.29 ps |
| Sampling diode | 1•3 μm | 1•1 μm |
| Differentiator | 1.0 ps | 0.5 ps |
| Net Sampler time (SPICE) | 0.5 ps | 0.3 ps |

Figure 2: Summary of design parameters for the 515 GHz and 725 GHz NLTLs & Sampling circuits

As line parasitics are most important where the conductors are narrow and where the Bragg frequencies are high, air-bridge-lines must be used near the NLTL output. Conventional air-bridges processes (as used for example in the Stanford designs) are too large (5-10 μm minimum dimensions) to use near the NLTL output. Instead, in the present contact period we developed a modified fabrication process whereby the signal conductor has its normal support posts eliminated. Instead, the air-bridge-line is supported by directly contacting the top of the Schottky diode contacts. The support-post capacitance is eliminated; metal contacts semiconductor only in the diode active areas.

A sophisticated process was required for fabrication of these low-loss lines. After deposition and annealing of the ohmic contacts, the Schottky contacts were deposited by liftoff. The wafer was then covered by a thick layer of Polyimide. The polyimide is subsequently etched in an oxygen reactive-ion-etching system until approximately 0.2 μm of the Schottky metal is exposed. The remaining process is similar to a normal air-bridge fabrication process. Air-bridge posts for the elevated lines are formed on top of the polyimide and provide contacts to the tops of the diodes. After electroplating the elevated lines the polyimide is removed, leaving the contacts between the CPW and the diodes in air, substantially reducing the parasitic layout capacitance.

Figure 2 (above) summarizes the expected improvement in performance with the new NLTL and sampling circuit designs. Measured NLTL skin-effect losses are reduced by approximately 4 dB. Further, loss in amplitude of the shock-wave with propagation distance is compensated for by impedance tapering. The net reduction in signal amplitude during propagation on the NLTL is therefore greatly reduced.

While it was expected that the newer NLTL designs would show significantly improved performance from improvements in the transmission-lines alone, improvements in the diode technology were also pursued. These efforts were less successful. Several diode structures were pursued, including GaAs/AlGaAs heterojunction barrier Schottky varactor diodes, and stacked-epitaxial diode designs in which several different diodes designs could be incorporated in different portions of the NLTL. While design of the GaAs/AlGaAs heterojunction barrier varactor diodes was described in the last contract report, processing and fabrication of such diodes continued throughout the period covered in the present report. With such diodes, the wide-bandgap AlGaAs cap layer potentially provides high reverse breakdown voltages despite the use of very thin diode layers as required for high cutoff frequencies. Extensive process runs with AlGaAs/GaAs diodes failed to produce reproducible diodes, a result ascribed to the ease with which AlGaAs can be oxidized or inadvertently etched by normal processing chemicals. The effort was eventually abandoned when it became apparent that the associated processing difficulties incurred were out of proportion to the expected improvements in performance.

Instead, heavily-doped, 1-μm-geometry GaAs Schottky diodes were employed. Circular diode geometries used in the sampling circuit and near the NLTL output allowed diode cutoff frequencies as high as 5 THz. Initial sampling circuits processed with this diode design had 725 GHz bandwidth (fig. 4). The measured 0.48 ps NLTL falltime closely correlated with that expected due to electron velocity saturation within the NLTL's Schottky varactor diodes.

Consequently, following the measurement of the 725 GHz / 0.48 ps result, 3 additional NLTLs designs were designed and fabricated using modified diode epitaxial designs. Diodes were more heavily doped, so as to decrease the depletion edge movement and thereby decrease the effect of velocity saturation. Patterned etching of the diode active layers was used to delineate different diode characteristics at different portions of the NLTL, exchanging as appropriate diode bandwidth against diode breakdown voltage. Despite these efforts, bandwidths above 725 GHz were not obtained. It is suspected that there are layout difficulties in the sampling circuit which are presently limiting the bandwidth. We believe that NLTL and sampling circuit bandwidths can be further extended to nearly 2 THz, but development of Schottky-Collector Heterojunction Bipolar Transistors (discussed subsequently) became a higher priority under the AFOSR program.

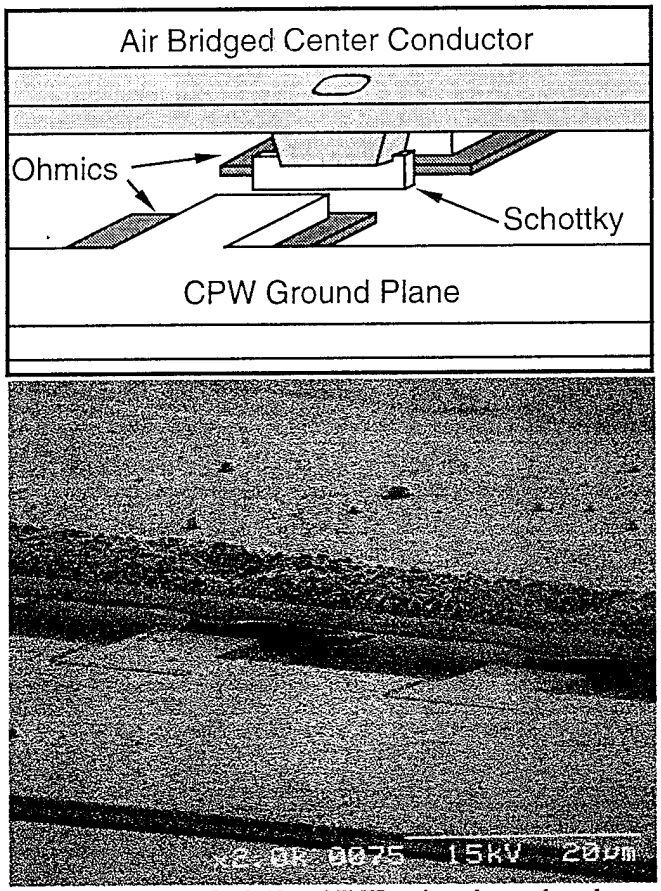


Figure 3: Diagram and SEM of a 0.48-ps NLTL using elevated coplanar waveguide.

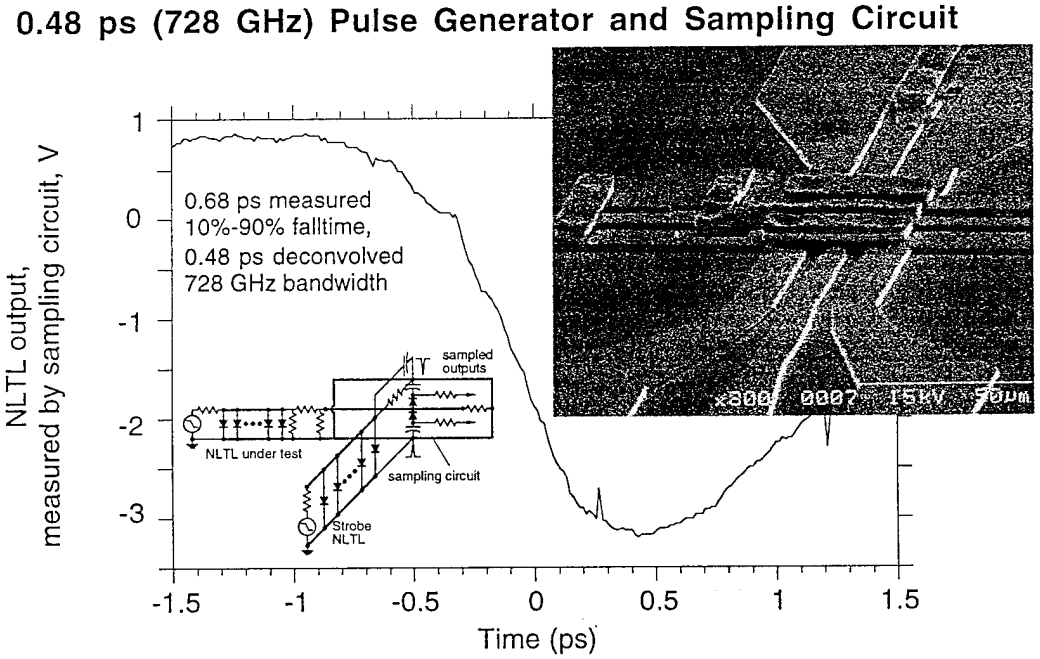


Figure 4: Circuit diagram, SEM, and measured waveform for a deep subpicosecond NLTL pulse generator and NLTL-gated sampling circuit.

Schottky-collector Bipolar Transistors

An emerging focus of the AFOSR contract is development of Schottky-collector heterojunction bipolar transistors (SCHBTs). Initial design calculations indicated that SCHBTs have potential cutoff frequencies in the 500-1000 GHz range. There is a very large potential impact on future millimeter-wave systems, with the strong possibility of sophisticated transistor integrated circuits replacing the elementary waveguide-coupled diode technology currently used at higher mm-wave frequencies. Because of the very high potential bandwidth they offer in a 3-terminal device SCHBTs became the major focus of the AFOSR program in its last 12 months

*Technical Description*

SCHBTs are HBTs modified so that the collector and emitter widths can be scaled to below 0.1 μm width. Transistor cutoff frequencies of 500-1000 GHz become feasible. The SCHBT technology has two key features: an epitaxial transfer process to allow lithographic definition of both the emitter and collector (thus removing excess base-collector capacitance), and Schottky collector contacts to allow scaling of the collector contact dimensions to 0.1 μm.

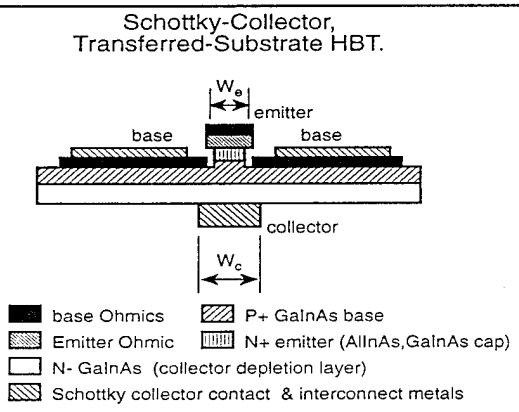


Figure 5: SCHBT cross-section

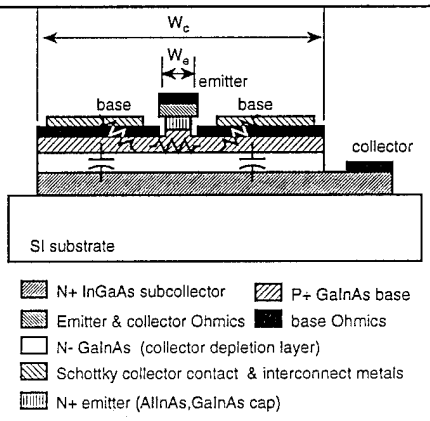


Figure 6: Normal HBT cross-section

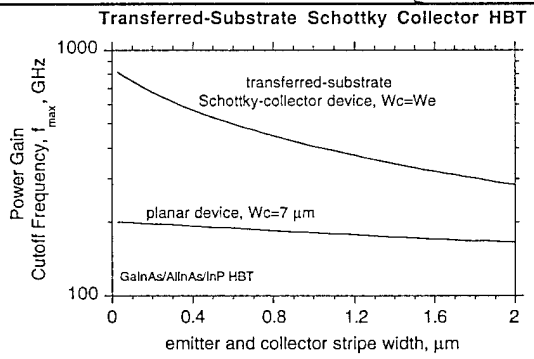


Figure 7: SCHBT and HBT bandwidth versus lithographic minimum feature size

The SCHBT obtains a large reduction in a resistance-capacitance time constant, hence a large increase in $f_{max}$, by extreme scaling through the use of a deep-submicron Schottky-collector-contact. Conventional HBTs do not benefit from submicron scaling of lithographic dimensions. With the SCHBT, two key innovations result in greatly improved bandwidth during scaling: a substrate transfer during processing which allows lithographic definition of narrow collectors and emitters, and a submicron Schottky collector contact which permits scaling to 0.1 μm width. Simultaneously scaling the SCHBT emitter and collector stripe widths from 1 μm to 0.1 μm results in a dramatic reduction in $r_{bb}C_{cb}$, increasing the transistor power-gain cutoff frequency $f_{max}$ to nearly 1000 GHz. This is explained below. The approach is a direct application of scaling laws, with no new device physics.

First consider HBT bandwidth. While $f_\tau = 1/2\pi(\tau_b + \tau_c)$ depends only on transit times, $f_{max} = \sqrt{f_\tau / 8\pi R_{bb} C_{cbi}}$ involves the base resistance and the internal collector-base capacitance $C_{cbi}$. High-speed circuits require that $f_{max}$ $and$ $f_\tau$ be high, with a 1.5:1 $f_{max} : f_\tau$ ratio generally optimum.

Figs. 5 & 6 show comparative cross-sections of HBTs and SCHBTs. In the normal HBT the collector junction width $W_C$ is much larger than the emitter stripe width $W_e$, greatly increasing $C_{cb}$ and decreasing $f_{max}$. More important, the scaling properties of normal HBTs are ruined by the large collector junction. The collector-base capacitance $C_{cb}$ is proportional to the collector width but is independent of the emitter width. The base resistance is dominated by the base ohmic contact resistance and is consequently independent of the emitter width for emitter widths below ≈2 μm. Since $f_\tau$ and $r_{bb}C_{cb}$ are independent of the emitter width, so is $f_{max}$. For emitter stripe widths below 1 μm, $f_{max}$ does not improve.

In contrast, SCHBTs have a collector contact width equal to the emitter width. This results in smaller $C_{cb}$ and a significant increase in $f_{max}$. More importantly, deep submicron scaling greatly increases the bandwidth of SCHBTs. $C_{cb}$, proportional to the collector width, is proportional to the emitter width since the widths are now equal. The base resistance is still independent of emitter width, and hence $r_{bb}C_{cb}$ is proportional to the (equal) emitter and collector widths. Consequently, $f_{max} \propto 1/\sqrt{W_C}$ : the device bandwidth varies as the inverse square root of the lithographic dimensions. At 0.1 μm critical feature sizes, cutoff frequencies above 700 GHz result, well above the present art for HBTs. The $f_{max}$ calculations of fig. 7 use InGaAs/AlInAs HBT material parameters from the literature.

There are limits to emitter and collector submicron scaling. As the emitter width is reduced, its periphery-area ratio increases and the current gain ß drops due to surface recombination at the emitter-base mesa edge. This can be controlled by proper surface passivation: AlGaAs/GaAs HBTs with 0.3 μm emitter width have recently been reported.

An efficient Schottky collector must be as wide as the emitter, and alignment tolerances must be accommodated. Because of fringing fields, the effective collector width is the physical collector width plus the collection depletion layer thickness. With a projection aligner, 0.5 μm features can be defined at 0.2 μm alignment tolerance. This limits the emitter width to 0.5 μm and the collector width to 0.9 μm, resulting in $f_{max}$=440 GHz.

With electron-beam lithography a 0.1 μm emitter and a 0.1 μm Schottky collector width are feasible, giving an $f_{max}$=750 GHz.

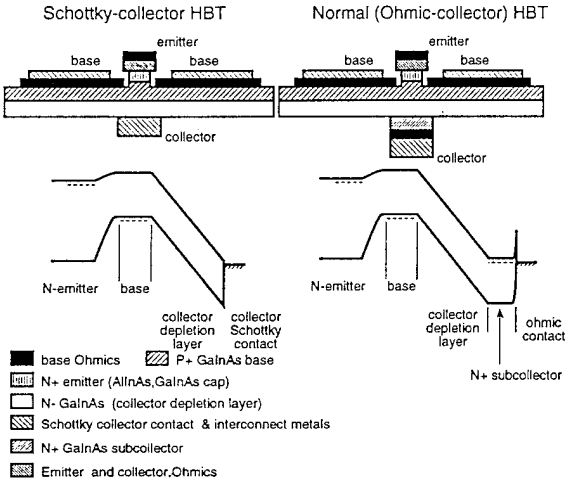


Figure 8: Layer Structures and band diagrams comparing ohmic- and SCHBTs

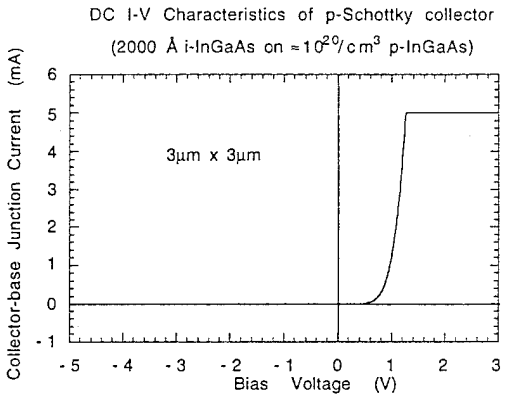


Figure 9: Measured characteristics of a InGaAs/InAlAs SCHBT collector-base junction.

Fig. 9 compares the band diagrams and layer structures of Schottky-collector vs. a transferred-substrate HBT using a normal ohmic collector. The Schottky collector enables lithographic definition of collector contact widths as small as 0.1 μm. The ohmic collector requires several process steps for fabrication and is therefore more difficult to scale to 0.1 μm. In InGaAs/InAlAs SCHBTs the contact is to InGaAs. Schottky contacts to N-InGaAs result in very leaky junctions due to the small 0.2 eV *conduction-band barrier*, but it is the large 0.5 eV *valence-band barrier* which is relevant here; base/Schottky-collector junctions UCSB has fabricated have low measured reverse leakage (fig. 9).

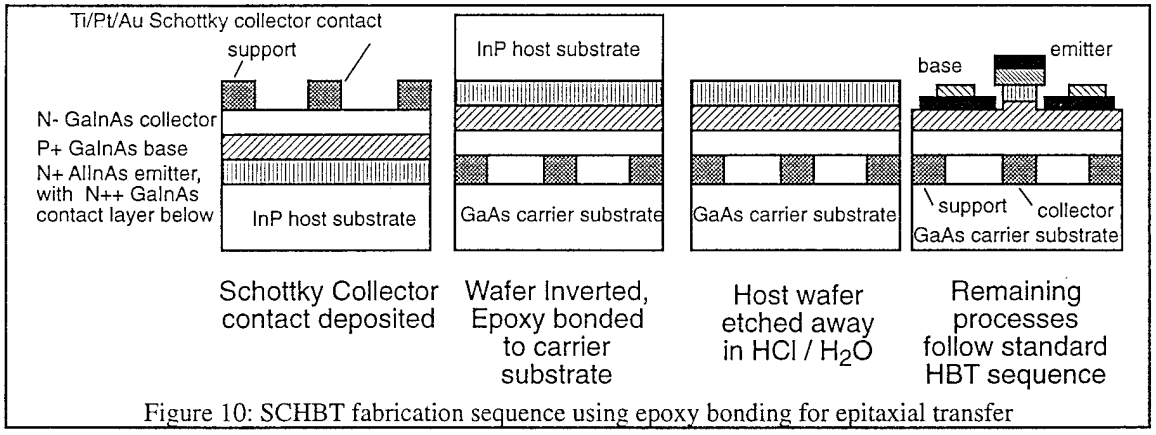


Figure 10: SCHBT fabrication sequence using epoxy bonding for epitaxial transfer

SCHBTs require high resolution processing of both sides of the transistor layers using epitaxial transfer. A process flow using epoxy adhesives is shown in fig. 10. While this process may seem aggressive, Rockwell Science center has demonstrated the transfer of 3 inch diameter AlGaAs HBT wafers to AlN and diamond substrates for improved heat sinking.

*Progress during the contract period*

During the contract period the following work was pursued. Initial design calculations and feasibility analysis were performed by one graduate student under AFOSR support. Initial designs had used a Schottky tunneling emitter in addition to the Schottky collector. The intent: the electrical dimensions of the tunnel emitter are the same as the Schottky contact footprint. Emitters with 0.1 μm width would therefore be easily obtainable by electron-beam lithography. Mask sets for this device were fabricated, and several InGaAs/AlAs wafers grown by MBE. Initial processing was then pursued. There were difficulties with the tunnel emitter which led to its abandonment after 2 months work: specifically, the graded tunnel barrier layers, having ≈100 Å thickness, were readily attacked and damaged during photolithographic processing steps.

Subsequently, we have focused on fabrication of a Schottky-collector HBT having a normal N+ emitter. N+ emitters are readily fabricated at 1 μm dimensions. Scaling of an N+ emitter to ≈0.1–0.2 μm emitters requires deposition of emitter ohmic contact metal with a subsequent self-aligned etch through the emitter using an RIE system. In early 1994, similar processing steps were demonstrated during the fabrication of Junction-High-Electron-Mobility-Transistors at UCSB. Success with this device was a strong indication of the feasibility of scaling SCHBTs to 0.2 μm dimensions whilst maintaining the N+ semiconductor emitter. The tunnel emitter was therefore abandoned in favor of the N+ semiconductor emitter.

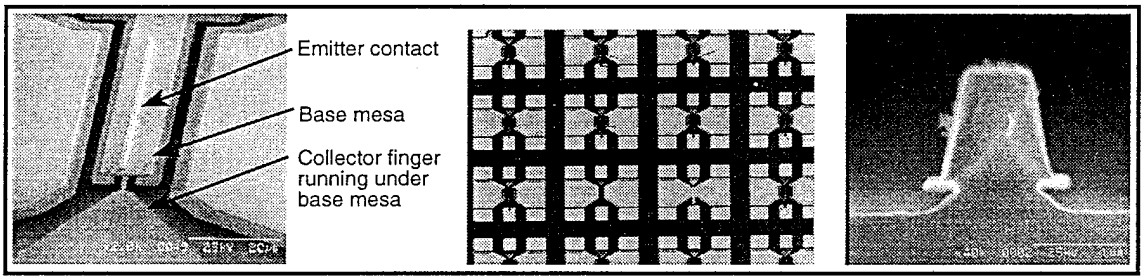


Figure 11: SCHBT before emitter planarization. Center: Array of processed devices. Right: Emitter cross-section.

Process development for 1-μm-geometry InGaAs/InAlAs SCHBTs was started in May 1994. A variety of epitaxial transfer technologies have been developed by Prof. Bower's group at UCSB, including Palladium bonding, epoxy bonding, and wafer fusion. Experiments performed in the Summer of 1994 indicated that epoxy bonding under vacuum, with the correct adhesives and curing, is remarkably robust under processing. While there was some concern regarding the poor thermal conductivity of the epoxy, electron micro graphs indicate that the epoxy is below 300 å thickness between the Schottky collector and the GaAs transfer substrate, and must therefore have a very low net thermal resistance. Further, the metal contacts to the collector and emitter have 6 times greater thermal conductivity than the GaAs substrate, and are very effective heat-spreading devices. Fabricated SCHBTs biased at normal power densities do not fail thermally, nor does the epoxy show evidence of thermal stress. Power dissipation is in the collector-base junction: it is likely that the superior thermal conductivity of the Schottky collector more than offsets the thermal resistance of the sub-300-å epoxy film.

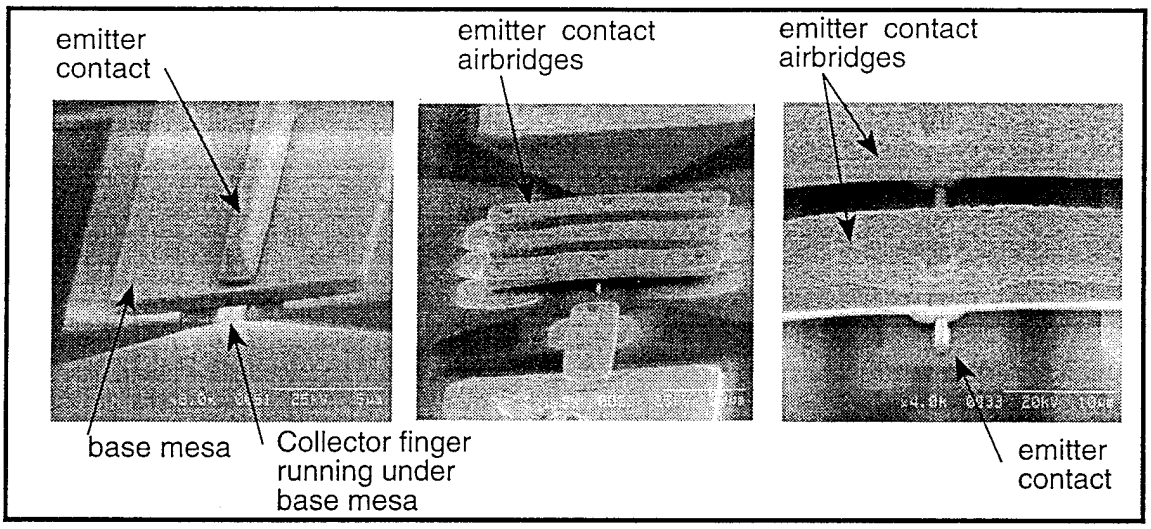


Figure 12: Left: SCHBT before emitter planarization. Center and Right: Views of completed device.

Three views of first-generation SCHBTs are shown in fig. 11. On the left is an SEM of a nearly-completed device, shown before emitter planarization for clarity. The center image shows an array of completed devices: on the 1 cm by 1 cm samples currently being processed, the epoxy bonding shows no defects. Samples will be scaled to 1-inch dimensions and larger as research processes from devices to circuits. The right SEM shows an emitter cross-section prior to base contact metal deposition. The self-aligned emitter-base process is high-yield but currently uses wet chemistry; dry etching in the UCSB facilities must be adopted as the emitter dimensions are scaled to below 1 μm.

Three additional images of SCHBTs are shown in fig. 12. The left image shows a high-magnification SCHBT image prior to emitter planarization. This device shows a slight collector misalignment: at UCSB, e-beam processes will be used to obtain submicron alignment precision. In industrial applications, 0.1 μm registration can be obtained using projection aligners, a resource presently unavailable at UCSB. The center and right images show the completed SCHBT after polyimide planarization/passivation and formation of emitter contact airbridges.

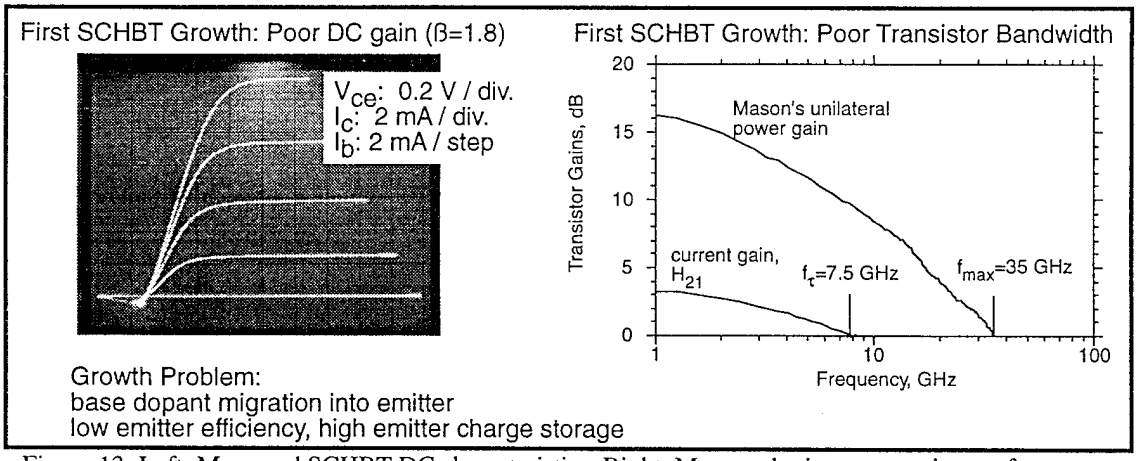


Figure 13: Left: Measured SCHBT DC characteristics. Right: Measured microwave gains vs. frequency.

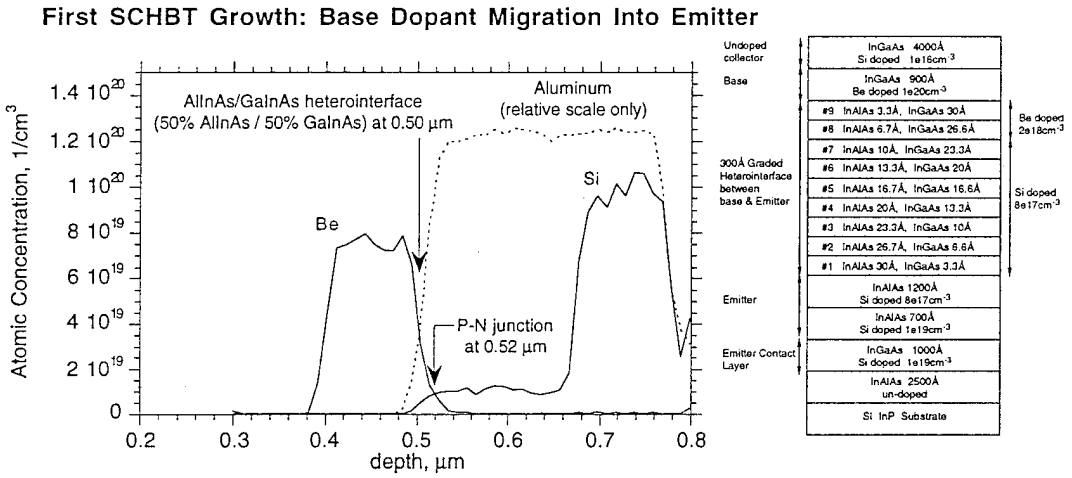


Figure 14: Doping profile of the first processed SCHBT wafer as measured by secondary ion mass spectrometry (SIMS). Base dopant diffusion has resulted in the emitter-base PN junction falling entirely within the wide-bandgap layer. Severe hole injection into the emitter results.

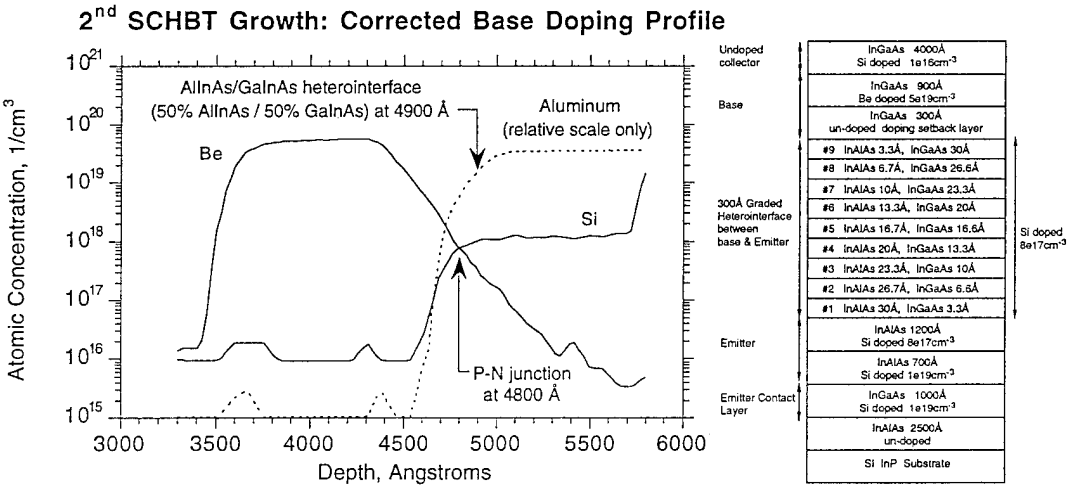


Figure 15: Doping profile of an SCHBT wafer with an improved base doping profile. Base doping was reduced to $5 \cdot 10^{19}$ /cm$^3$ , growth temperature reduced, and the base doping set back 300 å . The base-emitter p-n junction is now correctly located.

Figure 13 shows measured performance of the first SCHBTs, completed November, 1994. The devices show both extremely poor DC current gain and very poor bandwidth in relation to the expected ≈200 GHz. The origin of these difficulties is in the transistor materials growth. Figure 14 shows measured doping and alloy profiles of the first SCHBT, determined by SIMS. The target MBE growth profile is shown on the right of figure 14. The Be base dopant has diffused through the InGaAs/InAlAs base-emitter heterojunction, forming a P-N junction located within the wideband InAlAs emitter. This is a classical failure mode in HBT growth. The energy barrier blocking hole injection from base into emitter has been greatly degraded. There is consequently a very small DC current gain, and the substantial emitter stored (hole) charge results in a very low current-gain cutoff frequency.

Since November, research has focused on resolving improving growth and fabrication processes, particularly the base dopant migration. A variety of MBE growths have been performed, varying base doping, growth temperature, and base doping setback. All growth were characterized by SIMS. Fig. 15 shows the MBE target growth profile and SIMS data (doping profile) for an growth performed in January 1995. The P-N doping transition has penetrated only 50 å into the 300 å InGaAs/InAlAs graded emitter-base heterojunction. A caution should be made: the spatial resolution of SIMS analysis is such that is useful only as a first indicator of base dopant migration. In subsequent growths, the migration of base dopant is monitored by measurements of the base-emitter turn-on voltage (e.g. the so-called Gummel plot), which is very sensitive to this parameter. Devices processes on this wafer had a greatly increased power-gain cutoff frequency, as shown in figure 16, below. SCHBTs with a 1-µm-wide collector obtained a 61 GHz power-gain cutoff frequency, 2.5:1 larger than reference wide-collector devices fabricated on the same wafer. The latter devices have a geometry almost identical to a normal HBT, and serve as a standard of comparison for the SCHBT. Despite this, unfortunately the DC current gain remained low at ß=2.7.

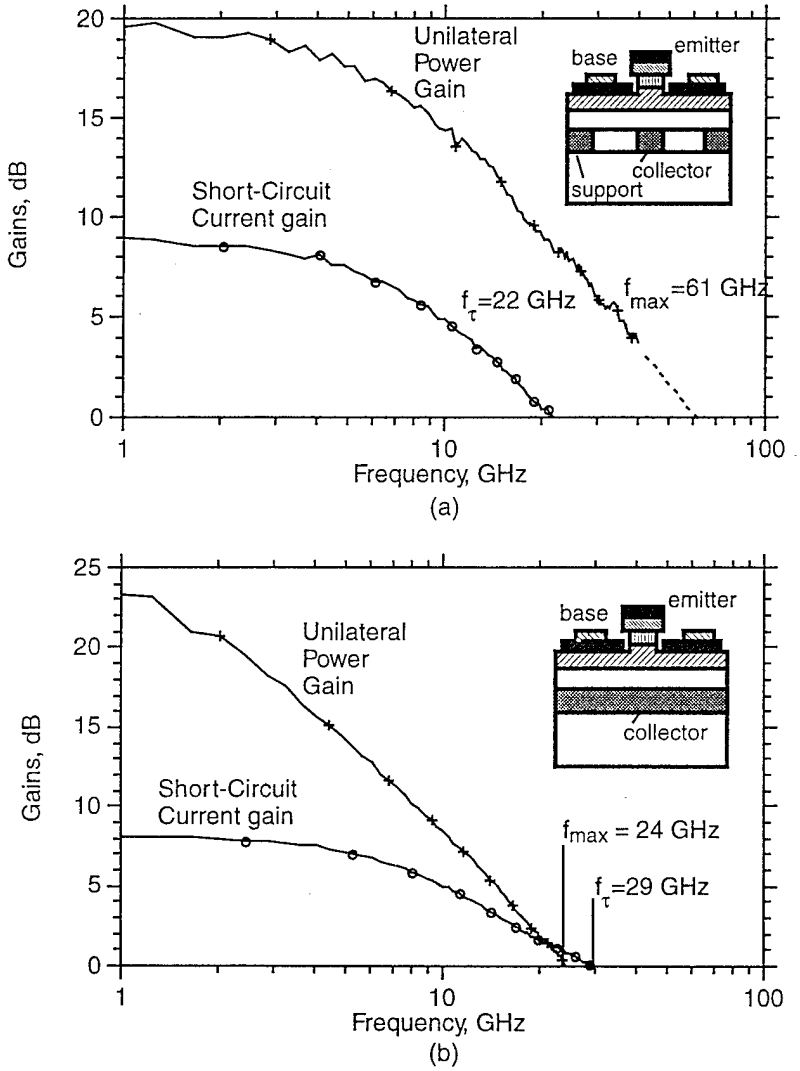


Figure 16: Comparison of the RF characteristics of (a) and SCHBT with 1-µm collector width to (b) a wide-collector reference device

Subsequent work has focused on improving the material epitaxial growth further. Base doping positioning relative to the emitter remains to be fully resolved, as excessive base migration into the emitter causes the catastrophic loss in gain described above, but insufficient movement of base dopant into the designed-in base dopant setback layer results in a retrograde base doping profile with both increased base transit times and decreased current gain. The additional major problem addressed over the course of the program period is vertical and lateral control of the base recess etch. Extremely precise vertical depth control is required in etching through the emitter to access the base because of the small 500-700 å base thickness. The degree of lateral etching is also a major issue, as excess lateral etching undercuts and destroys the emitter, while insufficient lateral etching of the emitter results in the base ohmic contacts being placed within an electron diffusion length of the emitter, whereby they act as very effective electron recombination centers, destroying the transistor' current gain. Gary Hurtz, a graduate student supported under the associated AASERT program developed an "umbrella" process which solved the latter problem (figures 17, 18). DC and RF characteristics of the resulting devices are shown in figures 19 and 20. The DC current gain is now 20-30, and the power-gain cutoff frequency exceeds 100 GHz.

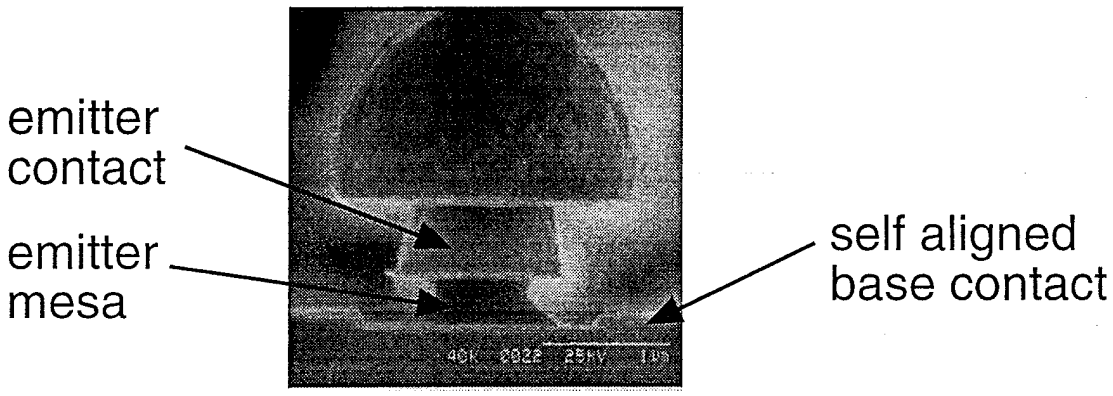


Figure 17: Emitter "Umbrella" Process developed by G. Hurtz. The plated cap on the emitter contact metal acts to prevent base contact metal deposition in direct contact with the emitter mesa. Subsequent processes with better emitter etch control did not require this feature.

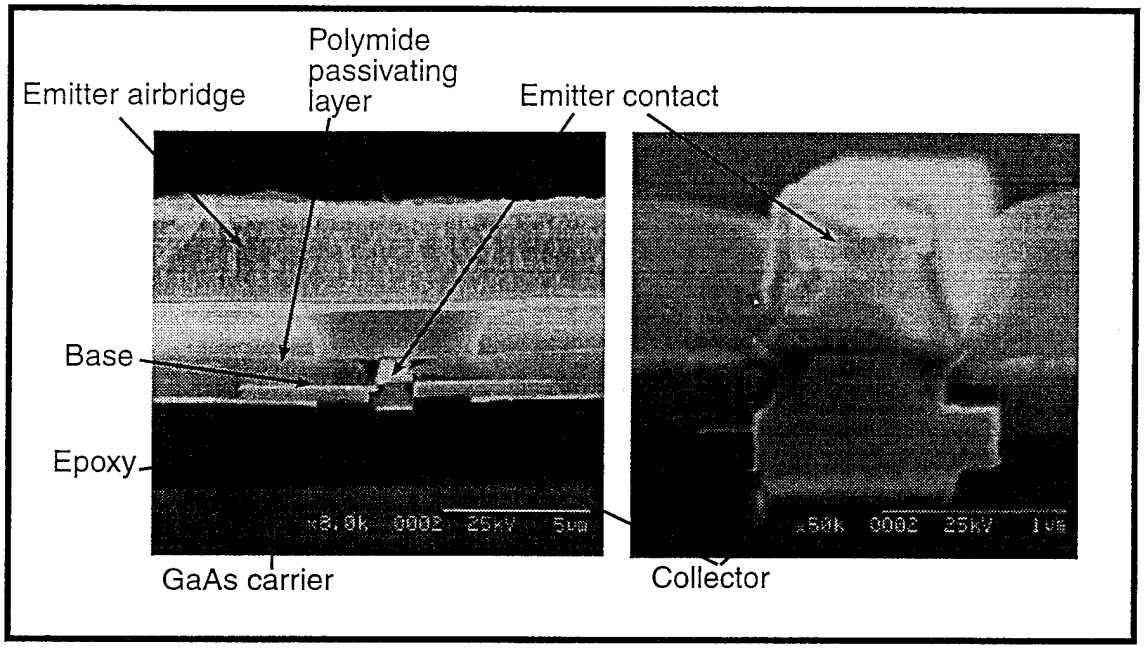


Figure 18: Cross-sections imaged by an electron beam microscope after cleaving. Note that the base contacts have fractured from the emitter/collector stripe during cleaving. The epoxy is abnormally thick on this process run.

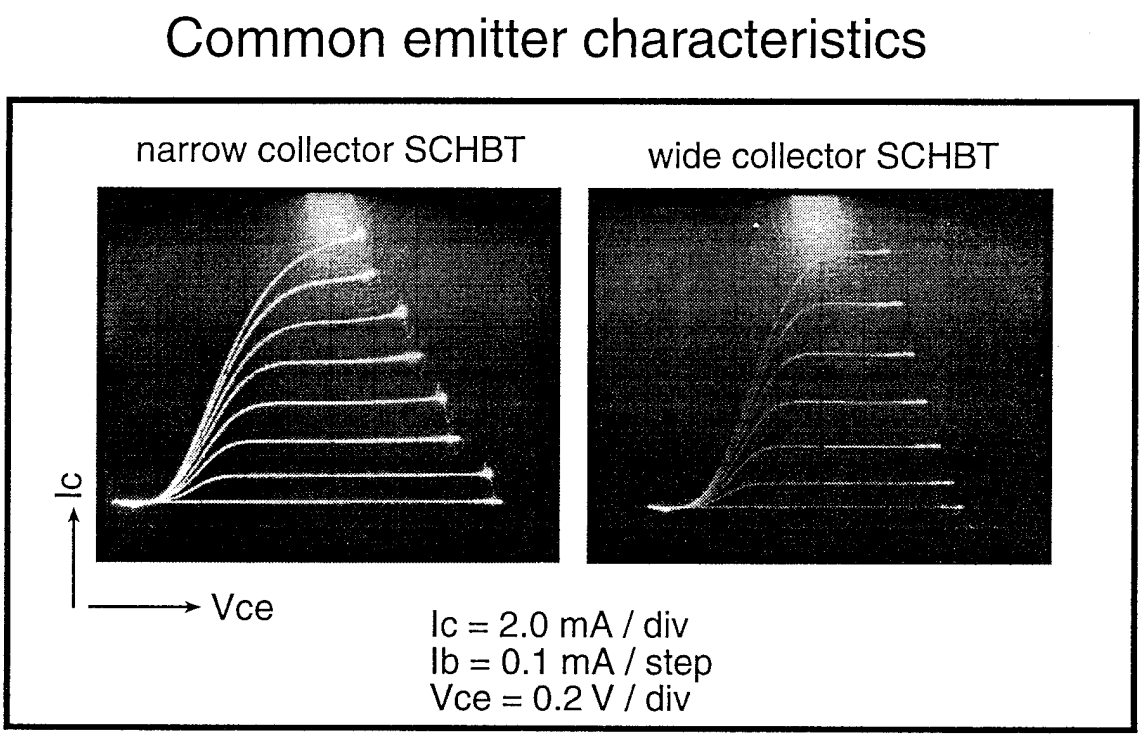


Figure 19: Measured DC characteristics of recent devices. The DC current gain is now 20-30.

## RF characteristics of SCHBT with $W_C = W_e = 1\mu m$

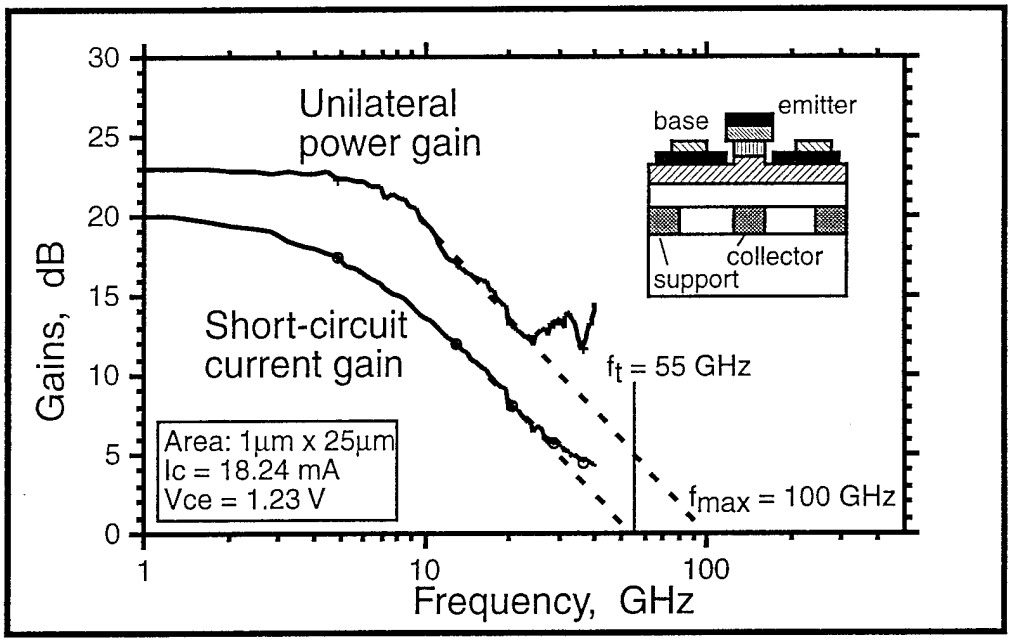


- $f_{max} / f_t = 1.8$

## RF characteristics of wide collector SCHBT

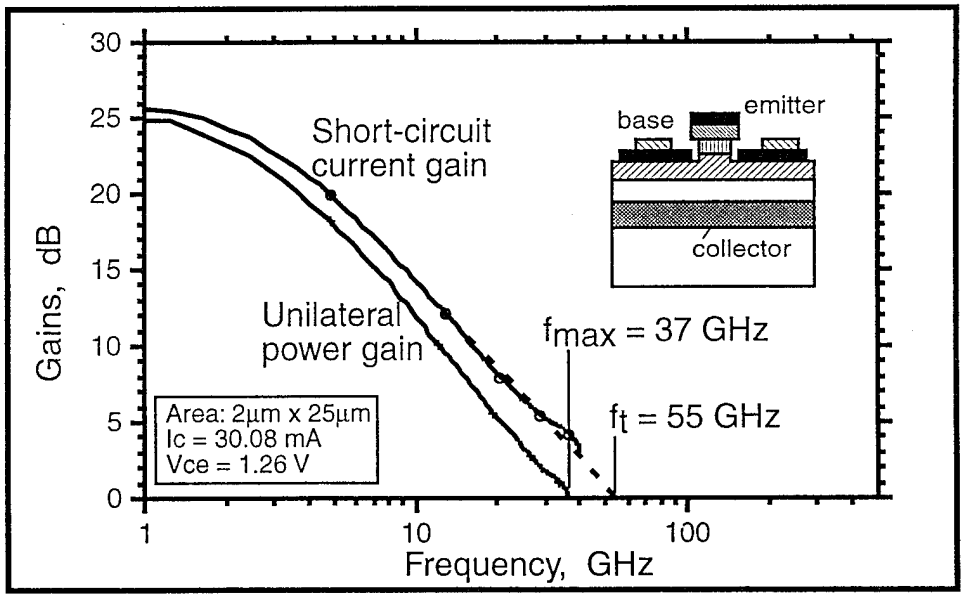


- reference device similar to normal HBT

Figure 20: Results as of program's end. Top: 1-μm SCHBT power and current gains Bottom: Results with wide-collector reference device.

The results clearly do not yet meet the program's objectives. A renewal to the AFOSR contract has been granted. Under this contract, the materials and process difficulties will be fully resolved and the device subsequently scaled to deep submicron dimensions. Bandwidths will then exceed 500 GHz.

Active Probes for on-wafer electrical measurements to 200 GHz

A second major effort under the present AFOSR program and its associated AASERT contract was the development of millimeter-wave and picosecond electronic instrumentation based upon NLTLs. Based upon lower-performance versions of the NLTL and sampling circuits, full integrated circuits were developed for network analysis. These consisted of an NLTL pulsed stimulus signal generator, and an NLTL-gated directional sampling circuit used to independently measure the incident and reflected waves from the device under test.

For on-wafer measurements, active probes were constructed (fig. 21). These consisted of the NLTL-based active probe IC, a microwave signal-routing substrate, and a low-loss quartz coplanar-waveguide probe tip providing a DC-250 GHz connection to the device under test. During the AFOSR program, three generations of active probes were developed, with progressively improved IC and probe tip designs. A full system for on-wafer S-parameter analysis was constructed, with accuracy sufficient for circuit characterization to 200 GHz (figs. 22, 23). In addition to efforts in developing the probe hardware, obtaining operation to 200 GHz required substantial efforts in system design.

At the time of the last contract report, the active probe system provided usable gain-frequency measurements to 160 GHz. During the present program period, this was extended to 200 GHz, and the active probe system was demonstrated on a variety of high-speed and microwave integrated circuits. Improvements necessary to improve the usable bandwidth to 200 GHz were mostly at the system level. Signal processing electronics at the probe IF (sampled, low-frequency) outputs was improved to allow for higher sampled frequencies, a modification which reduces the effects of signal generator phase noise on measurement accuracy. Directivity of the system was improved by adding signal sum-and-difference operations prior to analog-digital conversion. Finally, the probe tip design was revised: earlier probe tips had a mask layout defect which resulted in trapping of polyimide processing residues on the probe tips, degrading their high-frequency performance. Resulting performance of the active probes is shown below in figure 24.

Having demonstrated raw system performance, the system was demonstrated through measurements of a number of microwave integrated circuits. Figures 24 and 25 below show measurements by the active probe system of AlGaAs/GaAs microwave ICs provided to UCSB by the Fraunhofer institute in Germany. Correlation between the UCSB probe system and a customized commercial system was within the expected range, given differences between circuits tested at the 2 locations.

More significantly, the active probe system has allowed development at UCSB of monolithic circuits with record performance. Complementary to the AFOSR-funded efforts in mm-wave measurements, monolithic amplifiers with c.a. 100 GHz bandwidth were developed. This program was a partnership between UCSB and Hughes Malibu Research Labs, with support provided by a MICRO contract jointly funded by the State of California and Hughes, by the AFOSR, and (recently) by ARPA. Circuits were designed at UCSB, fabricated at Hughes, and tested by the UCSB active probe system. The resulting

capacitive-division distributed amplifiers obtained a record 340 GHz gain-bandwidth product (fig. 26) , and circuits which should obtain substantially wider bandwidth are currently in fabrication. Significant to this work was the use of capacitive division: while capacitive division has been introduced by others, the improvements in gain-bandwidth products obtainable by this technique do not seem to have been recognized in the literature.

Finally, the active probes have been used to characterize NLTL-based multiplexer-demultiplexer ICs for 100 Gbit/s fiber-optic transmission, ICs developed under the ARPA-funded Thunder & Lightning program (fig. 27). The active probes continue to be key resources for mm-wave IC development: UCSB/Hughes monolithic amplifier IC designs are in fabrication with target 200 GHz bandwidth. These are to be tested on the active probe system.

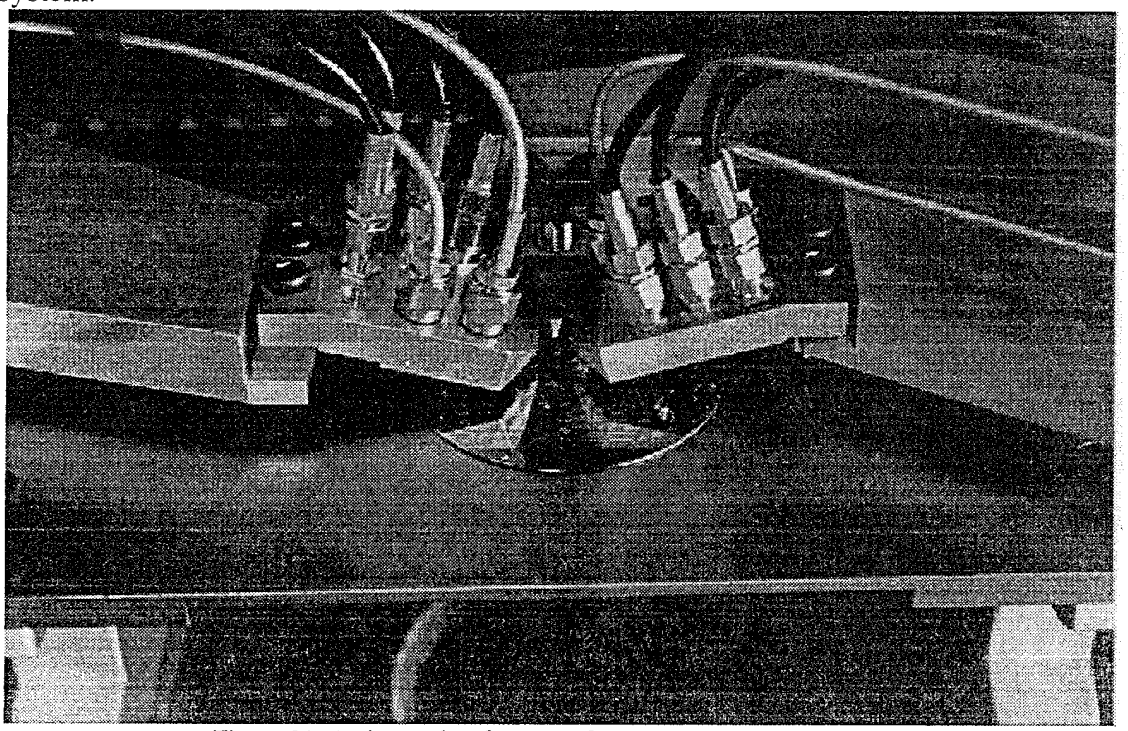

Figure 21: Active probes for on-wafer mm-wave network analysis.

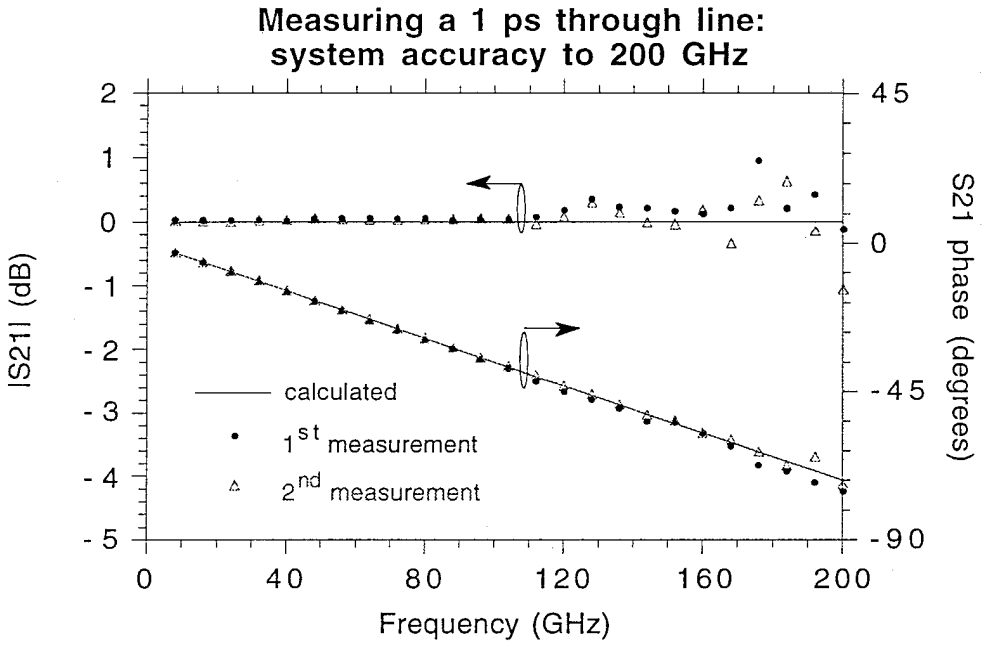


Figure 22: Verifying probe performance. Measured 7-200 GHz characteristics of a 1-ps-long 50 Ω through line 30 minutes after calibration. The transmission should be 0 dB at 1 ps delay.

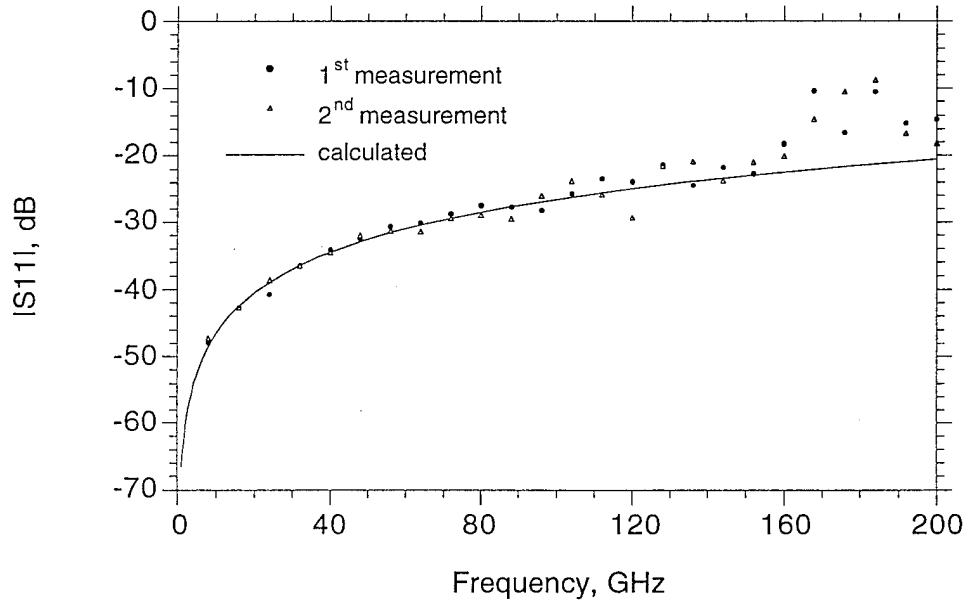


Figure 23: Verifying probe performance. Measured 7-200 GHz characteristics of a 50 Ω termination 30 minutes after calibration. Because of the finite load inductance, the reflection magnitude should be as indicated on the graph, not zero (-∞ dB).

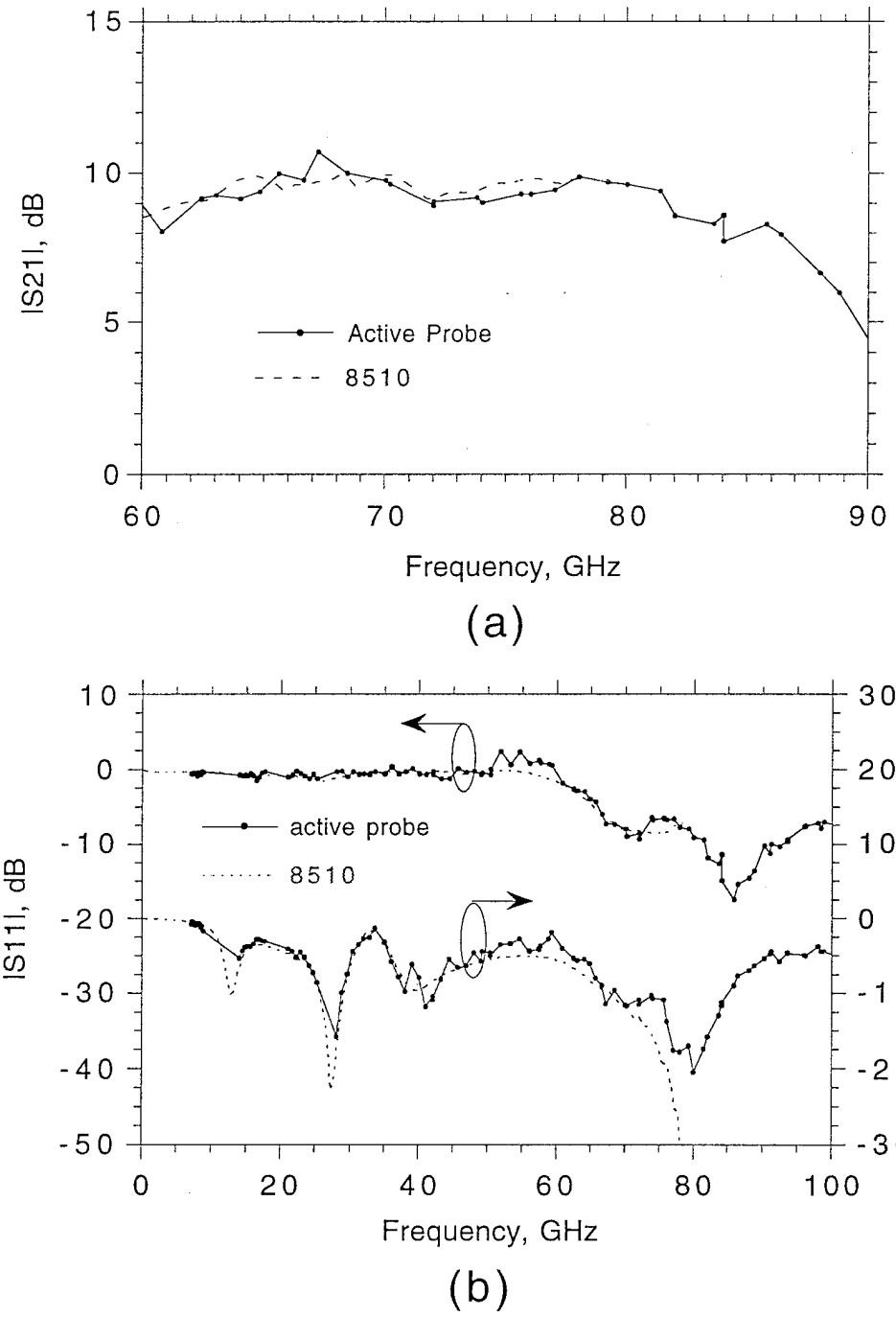


Figure 24: Gain (a) and reflection coefficients (b) of a medium-power V-band monolithic amplifier characterized by the active probe system. The amplifier was provided by the Fraunhofer Institution.

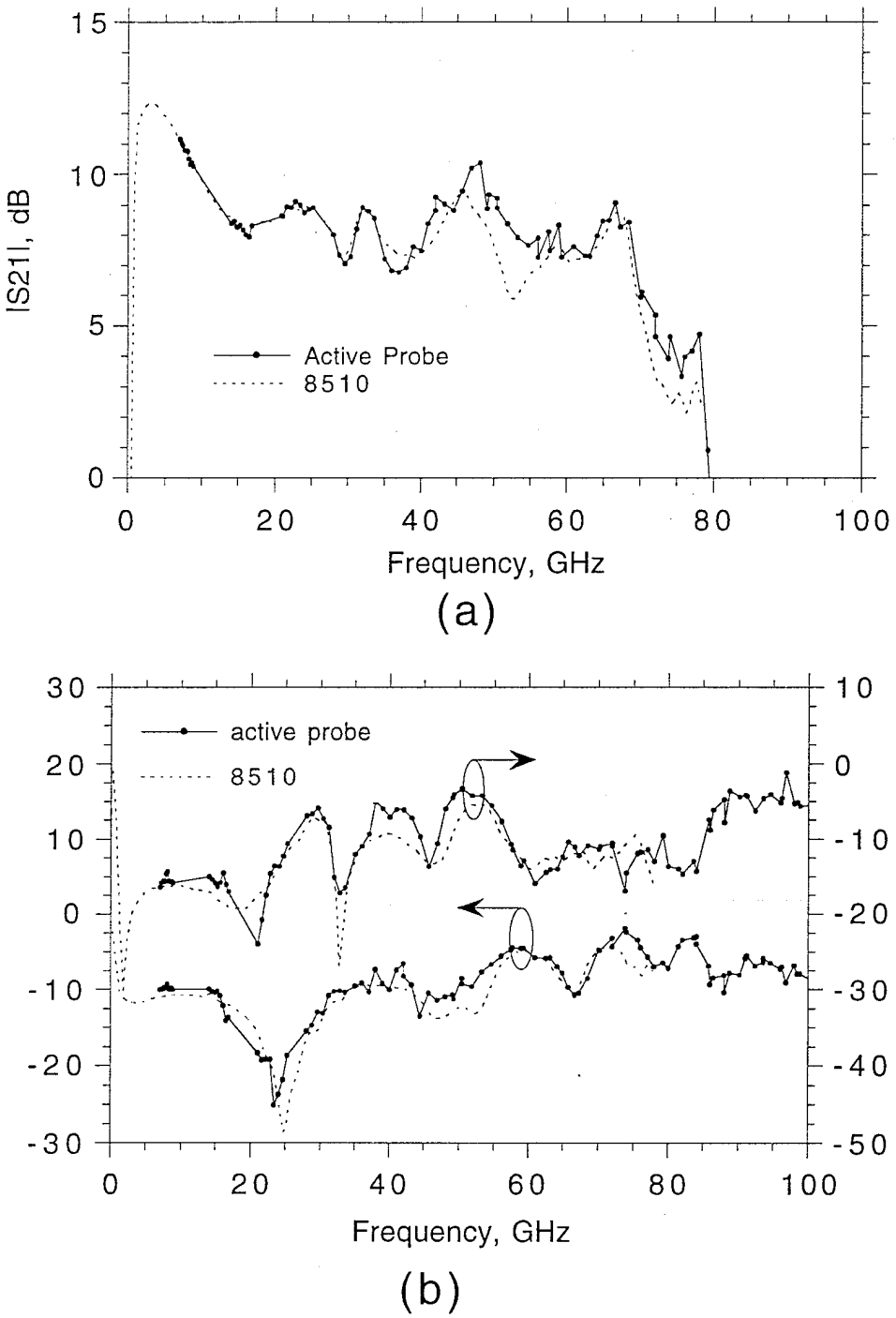


Figure 25: Gain (a) and reflection coefficients (b) of a monolithic traveling-wave amplifier characterized by the active probe system. The amplifier was provided by the Fraunhofer Institution.

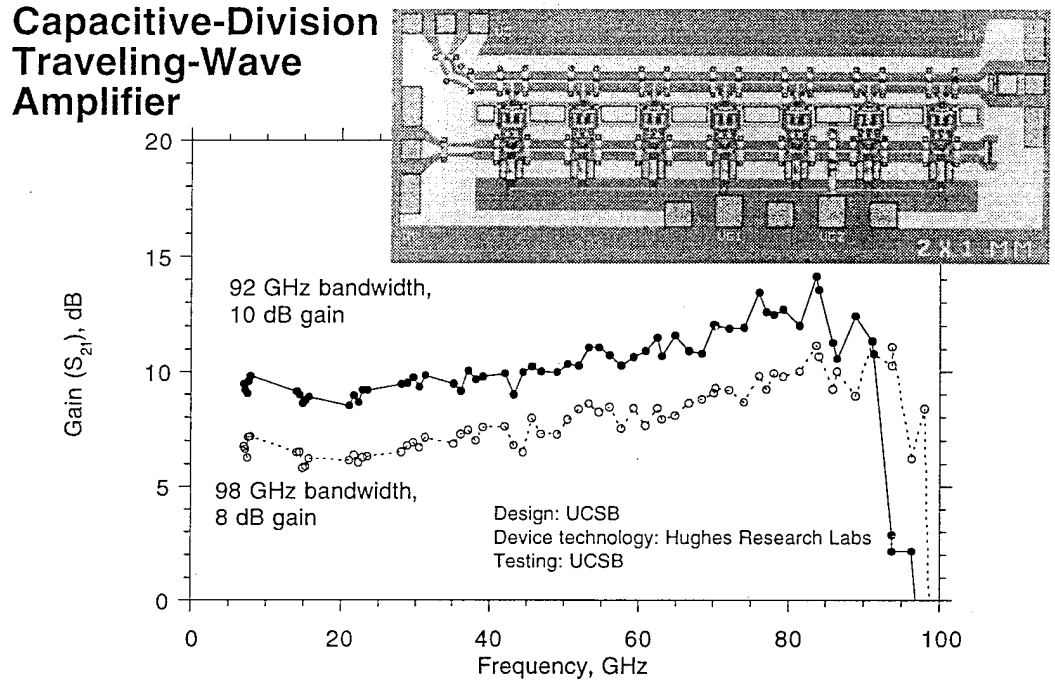


Figure 26: Gain vs. frequency for a UCSB/Hughes Amplifier, as measured by the active probe system

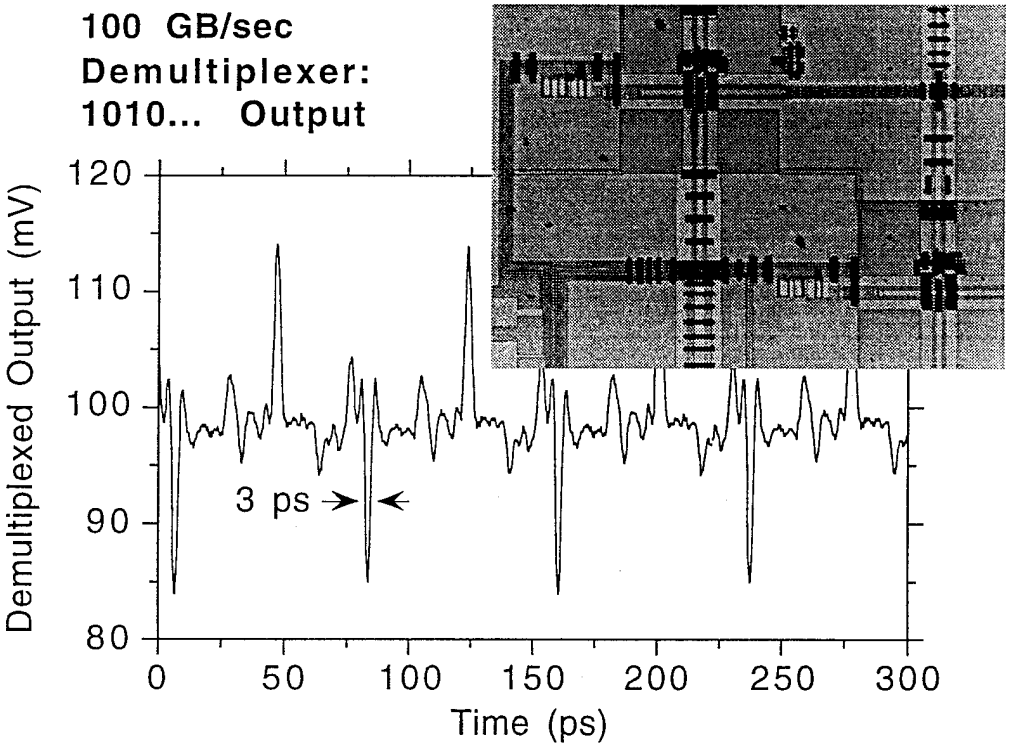


Figure 27: Output of a 100 Gbit/s demultiplexer as measured by the active probe system

## List of Personnel and Degrees

Principal investigator:
Mark Rodwell,
Department of Electrical and Computer Engineering
University of California, Santa Barbara, CA 93106

Graduate Students Supported:

1) Michael Case (AASERT program until June 1993)
Ph.D. received June 1993

2) Scott Allen (AASERT program from July 1993 to July 1994)
Ph.D received June 1994.

5) Gary Hurtz, (AASERT program September 1994 to August 1995)
M.S. received September 1995.

## Consulting and Advisory Functions

Consultant to Hughes Malibu Research Labs in the area of microwave transistor circuit design.

## Inventions and Patent Disclosures

To date, no patents have been filed.

## List of Written Publications in Technical Journals

| | | |
|---|---|---|
| Y. Konishi, M. Kamegawa , M. Case, R. Yu, S.T. Allen, and M. J. W. Rodwell, "A Broadband Free-Space Millimeter-Wave Vector Transmission Measurement System", IEEE Trans. MTT, Vol. 42, No. 7, July 1994, pp. 1131-1139. | IEEE Transactions Microwave Theory & Techniques | Journal Paper |
| S.T. Allen, U. Bhattacharya, M.J.W. Rodwell: "4 THz Sidewall-Etched Varactors and their application in Sub-mm-Wave Sampling Circuits", Electronics Letters, Vol. 29, No. 25, 9 December 1993, pp. 2227-2228 | Electronics Letters | Journal Paper |
| M.J.W. Rodwell, S. T. Allen, R. Y. Yu, M. G. Case, M. Reddy, E. Carman , J. Pusl, M. Kamegawa, Y. Konishi, and R. Pullela, "Active and Nonlinear Wave Propagation Devices in Ultrafast Electronics and Optoelectronics", Invited Paper, IEEE Proceedings, Vol. 82, No. 7, July 1994, pp. 1037-1058. | IEEE Proceedings | Invited Journal Paper |

| | | |
|---|---|---|
| R. Y. Yu, M. Reddy, J. Pusl, S.T. Allen, M.G. Case, and M.J.W. Rodwell, "Millimeter-Wave On-Wafer Waveform and Network Measurements Using Active Probes" IEEE Trans. MTT, Vol. 43, No. 4, April 1995, pp; 721-729 | IEEE Trans. MTT | Journal Paper |
| U. Bhattacharya, S.T. Allen, and M.J.W. Rodwell, "DC-725 GHz Sampling Circuits and Subpicosecond Nonlinear Transmission Lines Using Elevated Coplanar Waveguide", IEEE Microwave and Guided Wave letters, Vol. 5, No. 2, Feb. 1995, pp. 50-52 | IEEE Microwave and Guided Wave letters, | Journal Paper |
| U. Bhattacharya, M. J. Mondry, G. Hurtz, I. Tan, R. Pullela, M. Reddy, J. Guthrie, M. J. W. Rodwell, J. E. Bowers, "Transferred-Substrate Schottky-Collector Heterojunction Bipolar Transistors: First Results and Scaling Laws for high fmax", IEEE Electron Device Letters, Vol 16, No. 8, Aug. 1995, pp. 357-359 | IEEE Electron Device Letters | Journal Paper. |

## Papers Presented at Conferences

| | | |
|---|---|---|
| S.T. Allen, U. Bhattacharya, M.J.W. Rodwell: "4 THz Sidewall-Etched Varactors for Sub-mm-Wave Sampling Circuits", 1993 IEEE GaAs IC Symposium, October, San Jose, CA. | IEEE GaAsIC Symposium | Conference Paper |
| K S. Giboney, S. T. Allen, M. J. W. Rodwell, and J. E. Bowers, "1.5 ps fall-time measurements by free-running electro-optic sampling", 1994 IEEE/OSA conference on lasers and electro-optics (CLEO) | 1994 IEEE/OSA conference on lasers and electro-optics (CLEO) | Conference Paper |
| M.J.W. Rodwell, R. Yu, S. Allen, U. Bhattacharya, M. Reddy, 'Nonlinear Wave Propagation Devices for Ultrafast Electronics", Invited Paper, Conference on Ultra-Wideband Short-Pulse Electromagnetics, Weber Research Institute, Polytechnic University, Brooklyn, NY. 1994 | Conference on Ultra-Wideband Short-Pulse Electromagnetics, Weber Research Institute | Invited Conference Paper. |
| R. Y. Yu, M. Reddy, J. Pusl, S.T. Allen, M.G. Case, and M.J.W. Rodwell, "Millimeter-Wave On-Wafer Waveform and Network Measurements Using Active Probes", NASA/IEEE 5th international symposium on Space Terahertz technology, Ann Arbor, Michigan, May 1994 | NASA/IEEE 5th international symposium on Space Terahertz technology, Ann Arbor, Michigan, May 1994 | Conference Paper |

| | | |
|---|---|---|
| M. Schlectweg, W. Reinh ert, A. Bangert, J. Braunstein, P.J. Tasker, R. Bosch, W. H. Haydl, W. Bronner, A. Hulsmann, K. Kohler, J. Seibel, R. Yu, and M.J.W. Rodwell, "High Performance MMICs in Coplanar-Waveguide Technology for Commercial V-Band and W-band applications", 1994 IEEE Microwave and Millimeter-Wave Monolithic Circuits Symposium, May 22-25, San Diego | 1994 IEEE Microwave and Millimeter-Wave Monolithic Circuits Symposium | Conference Paper |
| M.J.W. Rodwell, R. Yu, M. Reddy, S. Allen, U. Bhattacharya, "Active Probes For On-Wafer millimeter-Wave Network Analysis", Invited Paper, IEEE Conference on Precision Electromagnetic Measurements, June 1994 , Boulder, Co. | IEEE Conference on Precision Electromagnetic Measurements, June 1994 , Boulder, Co. | Invited Conference Paper |
| S.T. Allen, U. Bhattacharya, and M.J.W. Rodwell, "725 GHz Sampling Circuits Integrated with Nonlinear Transmission Lines", presented at the 52nd annual IEEE Device Research Conference, Boulder, CO. June 1994. | IEEE Device Research Conference | Conference Paper |
| J. Pusl, B. Agarwal, R. Pullela , L. D. Nguyen, M. V. Lee, M. J. W. Rodwell, L. Larson, J. F. Jensen, R. Y. Yu, M. G. Case, "Capacitive Division Traveling Wave Amplifier with 280 GHz Gain-Bandwidth Product" Pusl et. al., "Capacitive-Division Traveling-Wave...", Presented at the 1995 IEEE MTT-S International Microwave Symposium, May 15-19, Orlando | 1995 IEEE MTT-S International Microwave Symposium | Conference Paper |
| U. Bhattacharya, M. J. Mondry, G. Hurtz, I. Tan, R. Pullela, M. Reddy, J. Guthrie, M. J. W. Rodwell, J. E. Bowers, "Schottky-Collector Heterojunction Bipolar Transistors: Device Scaling Laws for fmax beyond 500 GHz", Presented at the 1995 OSA Conference on Ultrafast Electronics and Optoelectronics, Dana Pt., CA, March | 1995 OSA Conference on Ultrafast Electronics and Optoelectronics, Dana Pt., CA, March. | Conference Paper |